

Multiple Ionization in Fast Ion-Atom Collisions: Simultaneous Measurement of Recoil Momentum and Projectile Energy Loss

M. A. Abdallah,* C. R. Vane, C. C. Havener, D. R. Schultz, H. F. Krause, N. Jones, and S. Datz
 Physics Division, Oak Ridge National Laboratory, Building 5500, P.O. Box 2008, Oak Ridge, Tennessee 37831-6377
 (Received 17 March 2000)

We report on the first experiment that measures simultaneously the full momentum vector of recoil ions and projectile energy loss and scattering angle in ion-atom collisions. We studied multiple ionization in the collisions of 0.83-MeV/u O^{7+} with Ne. Recoil ions (Ne^{q+} , $q = 1-8$) were detected in coincidence with single capture to O^{6+} . The results give the first experimental evidence for the increase of the average electron energy with increasing recoil charge state q . The average ejection angle shows a dramatic decrease with q . Results are compared with n -electron classical trajectory Monte Carlo calculations.

PACS numbers: 34.10.+x, 34.50.Fa

When a fast highly charged ion collides with a multielectron atom, several reaction channels can open simultaneously resulting in the ionization of several target electrons [1]. The projectile may interact with inner-shell electrons as well as outer-shell electrons by capture, excitation, or ionization. Also, electrons can be ejected to the continuum as a result of atomic rearrangement after the main collision. This simultaneous “activation” of many electrons in such collisions makes experimental and theoretical studies very difficult. Inner-shell processes, especially those with a K -shell vacancy, have received much recent attention [2]. However, those studies gave little information about the more probable outer-shell processes and therefore the collective nature of collisions. Questions such as what are the average energy and average ejection angle of the ejected electrons remained virtually uninvestigated.

To study the collective behavior of the ejected electrons, one has two options: measuring the momentum of *all* electrons in coincidence with recoil ions (and projectiles) or measuring the energy and momentum of recoil ions and projectiles. Although the simultaneous detection of two and three electrons has been reported [3–5], detecting all ionized electrons in a single collision remains virtually unachievable for higher degrees of ionization (target atoms which lost seven or eight electrons in a single collision are seen routinely). The second option is the more promising.

The lack of experimental data that give simultaneously recoil ion momentum and projectile energy loss was the motivation for the present experiment. Ignoring projectile deflection and applying conservation of momentum and energy, one can write the total longitudinal momentum of ejected electrons as follows:

$$\sum_{i=1}^n p_{e\parallel}^i = \frac{\Delta E}{v_p} - p_{r\parallel}, \quad (1)$$

where ΔE is projectile energy loss, v_p is projectile velocity, $p_{r\parallel}$ is the recoil longitudinal momentum, $p_{e\parallel}^i$ is the longitudinal momentum of the i th ejected electron, and n is the total number of ejected electrons. The relatively large projectile energy losses reported experimentally by Schuch *et al.* [6] and Schöne *et al.* [7] and also predicted

by sequentially bound n -electron classical trajectory Monte Carlo (n CTMC) calculations by Olson *et al.* [8,9] indicate that taking the projectile energy loss explicitly into account is important in calculating the average ejected electron momentum. The n CTMC calculations by Olson *et al.* [8–10] also predicted large ejection angles of the continuum electrons which makes a direct account of projectile energy loss even more important.

In general, projectile energy loss can be written as follows:

$$\Delta E = \sum_{i=1}^q U_i + E_b - \frac{1}{2}(q-n)v_p^2 + \varepsilon_{\text{ex}} + \sum_{i=1}^n E_e^i, \quad (2)$$

where the first term is the sum of the ionization potentials of the electrons lost by the target, the second term is the final energy of the captured electrons, the third term is the projectile kinetic energy change corresponding to the mass of the captured electrons [11,12], the fourth term is the excitation energy of the target and the projectile bound electrons, and the last term is the total kinetic energy of the ionized electrons. q is the total number of electrons lost by the target. The first, second, and fourth terms on the right-hand side combined are referred to as the Q value which represents the change in the electronic energy of the system [13]. Here we refer to the first four terms on the right-hand side of Eq. (2) as A . For single capture $q = n + 1$, and A is given by

$$A \equiv \sum_{i=1}^q U_i + E_b - \frac{1}{2}v_p^2 + \varepsilon_{\text{ex}}. \quad (3)$$

By calculating A and measuring projectile energy loss, one can determine the total kinetic energy of the ejected electrons [Eq. (2)]. Knowing the longitudinal momentum of recoil ions enables us to calculate the total longitudinal momentum of the electrons [Eq. (1)].

In this experiment we measure both recoil momentum and projectile energy loss. This was facilitated by using a cold-target recoil-ion momentum spectrometer [13] in conjunction with the high-resolution Elbek magnetic spectrometer [14] used in the earlier experiments [6,7]. In this

Letter we report on the study of multiple ionization accompanying single electron capture in the collisions of O^{7+} with Ne at an impact energy of 0.83 MeV/u. A detailed description of the experimental setup will be provided in a forthcoming publication [15]. Briefly, the O^{7+} beam was obtained from the ORNL EN Tandem. The Ne target was a supersonic gas jet precooled to about 70 K. The ion beam intersected with the gas jet at 90° . An electric field perpendicular to both beams was used to extract the recoil ions which, after passing through a field-free drift region, were detected by a two-dimensional position sensitive detector (2DPSD). Full momentum vectors of recoil ions were reconstructed from their positions on the 2DPSD and their time of flight [16]. After the collision the projectile ions entered the Elbek magnet which has inherent focusing capability in the dispersion plane. Using an appropriate magnetic field, oxygen ions which captured one electron (O^{6+}) were projected on a 2DPSD located on the magnet focal plane. The image on the detector was determined by projectile energy in the direction parallel to the dispersion plane and the scattering angle in the direction perpendicular to the dispersion plane [7].

In Fig. 1(a) we show the measured energy loss ΔE (solid squares), the term A (circles), and the total kinetic energy of the ejected electrons $\sum E_e^i$ (solid triangles) as functions of recoil charge state q . The latter quantity is compared to n CTMC [17] calculations (open triangles) in which all 11 target and projectile electrons are included with sequential binding energies given according to standard experimental

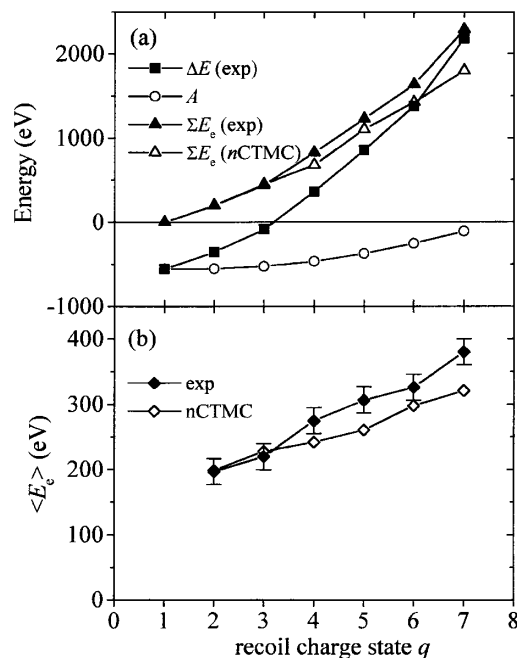


FIG. 1. (a) The term A (circles, see text), projectile energy loss (solid squares), ejected electrons total kinetic energy (triangles) in the collisions $0.83 \text{ MeV/u } O^{7+} + \text{Ne} \rightarrow O^{6+} + \text{Ne}^{q+} + (q-1)e^-$. (b) Average ejected electron kinetic energy as a function of recoil charge state q .

values. To calculate A , we ignored any excitation or inner-shell vacancy production that does not result in an Auger electron emission. This assumption is very accurate as the fluorescence yield for Ne ions does not exceed 0.2 even for ions with an empty $2p$ subshell [18]. The final state of the captured electron was taken as the average of the distribution of final n levels after single electron capture as a function of recoil charge state in the n CTMC calculations. The value of E_b was found to range from about -120 eV for Ne^+ to about -360 eV for Ne^{7+} as a result of capturing to deeper shells on the average in small impact parameter collisions. However, A is dominated by the captured electron mass term $-1/2v_p^2$ which is equal to -456 eV independent of the recoil charge state. As can be seen the kinetic energy of the ejected electrons accounts for the largest fraction of projectile energy loss especially at large recoil charge states. To determine the average energy of the ejected electrons we divide $\sum E_e^i$ by the number of ejected electrons ($q-1$). The resulting average kinetic energy $\langle E_e \rangle$ is shown in Fig. 1(b) along with the n CTMC result. It is noted that $\langle E_e \rangle$ increases with the recoil charge state, and is nearly doubled in going from $q=1$ to $q=7$. This behavior reflects the effect of impact parameter on the ejected electrons as small impact-parameter collisions result not only in higher degrees of target ionization, but also in larger average electron energies and the rise in Auger electron energies when K -shell electrons are removed either through ionization or capture. The large energy losses and average electron energies measured in this experiment are in qualitative agreement with previous experiments [6,7] and n CTMC calculations [8–10]. However, it should be noted that those n CTMC included all final projectile charge states (i.e., not restricted to single electron capture and consequently originating from a larger range of impact parameters than in the present experiment); therefore, caution should be taken when making direct comparisons.

In Fig. 2, we show the longitudinal recoil-ion momentum distributions where all distributions have been normalized to the same height and vertically shifted by equal amounts with respect to each other. The recoil momentum resolution for Ne^+ is about 0.9 a.u. and for Ne^{7+} is about 2.4 a.u. The distributions become wider with increasing q . Energy and longitudinal momentum of the ejected electrons are the major factors in determining the widths of these distributions. The position of the longitudinal recoil momentum peak does not show any dramatic shift and it is centered near $p_{r\parallel} = -2.5$. This backward “kick” to the target recoil is mostly due to a projectile energy increase that corresponds to the captured electron ($1/2v_p^2$) as reported by Frohne *et al.* [11,12]. From Eq. (1), we calculate the ejected electrons’ total longitudinal momentum. We divide the result by the total number of electrons in the continuum and show the result, $\langle p_{e\parallel} \rangle$, in Fig. 3(a). Since the distribution of energy and longitudinal momentum among the ejected electrons remains unknown, we get an estimate of the average transverse momentum of

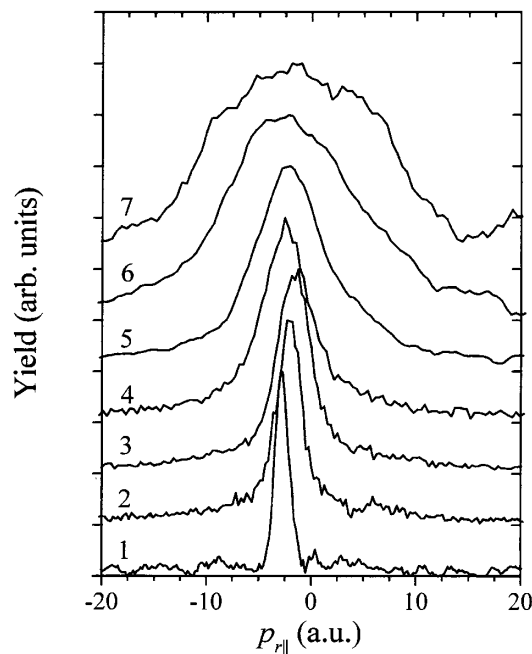


FIG. 2. Longitudinal momentum distributions of recoil ions produced in the collisions $0.83 \text{ MeV/u O}^{7+} + \text{Ne} \rightarrow \text{O}^{6+} + \text{Ne}^{q+} + (q-1)e^-$. Distributions are normalized to the same height and shifted equally from each other in the vertical direction. The number to the left side of each distribution refers to the corresponding recoil charge state q .

ejected electrons, $\langle p_{e\perp} \rangle$, using the following approximation: $\langle p_{e\parallel}^2 \rangle \approx \langle p_{e\parallel} \rangle^2$ and similarly $\langle p_{e\perp}^2 \rangle \approx \langle p_{e\perp} \rangle^2$. (We note that the n CTMC results yielded that $\langle p_{e\parallel}^2 \rangle \approx 2\langle p_{e\parallel} \rangle^2$ and $\langle p_{e\perp}^2 \rangle \approx 1.5\langle p_{e\perp} \rangle^2$.) Therefore, $\langle p_{e\perp} \rangle$ is given by

$$\langle p_{e\perp} \rangle \approx \sqrt{2\langle E_e \rangle - \langle p_{e\parallel} \rangle^2}, \quad (4)$$

and an estimate of the average electron ejection angle is given as

$$\langle \theta_e \rangle \approx \tan^{-1} \left\{ \frac{\sqrt{2\langle E_e \rangle - \langle p_{e\parallel} \rangle^2}}{\langle p_{e\parallel} \rangle} \right\}. \quad (5)$$

The approximate average transverse momentum and ejection angle of the continuum electrons are shown in Figs. 3(a) and 3(b), respectively, along with the n CTMC results computed using the calculated values of $\langle p_{e\parallel} \rangle$ and formulas (4) and (5). It is noted that $\langle p_{e\perp} \rangle$ is larger than $\langle p_{e\parallel} \rangle$ for all charge states. Both values increase with increasing recoil charge state, but the increase in $\langle p_{e\parallel} \rangle$ tends to be steeper especially at low q . Although the n CTMC calculations' prediction of the values of $\langle p_{e\perp} \rangle$ and $\langle p_{e\parallel} \rangle$ are in reasonable agreement with the experiment for high q recoils, it overestimates $\langle p_{e\parallel} \rangle$ for low q recoils. The strong decrease of the angle with increasing q can be understood as a direct measure of impact parameter. Relatively large impact parameter collisions result in the ejection of a few electrons at nearly 90° in dipolelike interactions. Harder collisions result in ejecting more electrons, on average, into smaller angles. This occurs due to dominance of forward binary collisions at small impact

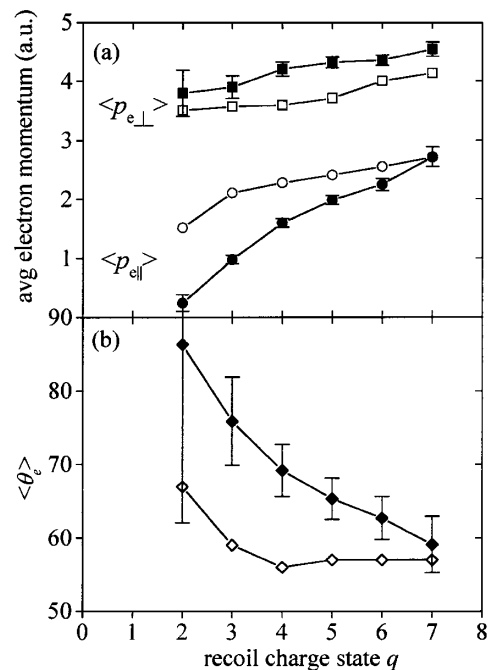


FIG. 3. (a) Average longitudinal momentum (circles) and average transverse momentum (squares) of the ejected electrons for the same collisions as in the previous figures. (b) Average electron ejection angle. In (a) and (b), solid symbols are from experiment and open symbols are from n CTMC calculations.

parameters, and to some extent because of the increasing role of the two center effects (postcollision interactions) as the electrons try to follow the highly charged projectile. Overall, the electrons are ejected preferentially in the forward direction as reported by previous experiments [4,11,12,19,20]. Inclusion of postcollision electron-electron interactions and a dynamic adjustment of the electron-ion (target and projectile) potentials presents a challenge for elaboration of the n CTMC model to try to more completely account for the observed behaviors.

Finally, we compare the full width at half the maximum (FWHM) for one component of the projectile (p_{px}) and the recoil (p_{rx}) transverse momentum distributions in Fig. 4. The difference between these two quantities is a direct measure of the contribution of ejected electrons in the momentum balance in the transverse direction. The projectile distributions have been corrected to account for the difference in experimental resolution between p_{rx} and p_{px} . For the recoil ions, the rapid increase in the distribution width and the large values of transverse momentum are in agreement with earlier measurements of Levin *et al.* [21]. We notice that the balance between recoils and projectiles in the transverse momentum is more dominant at larger recoil charge states which are produced in relatively close collisions and with less screening (two-body behavior). For small charge states, the contribution of the electrons in the momentum balance is important except for singly charged recoils where no electrons have been ejected to the continuum. In all cases the width for projectiles is smaller than recoils which indicates that in general

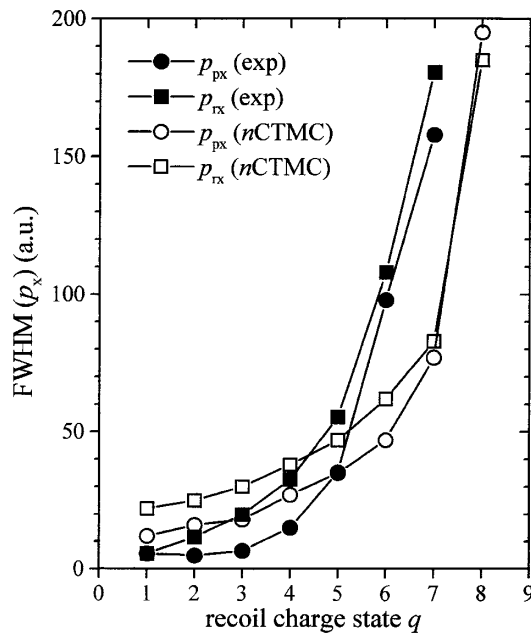


FIG. 4. The full width at half the maximum (FWHM) of one component of the transverse momentum distributions of recoils (p_{rx}) and projectiles (p_{px}).

the electrons prefer to be ejected away from the recoils and toward the projectile especially at low charge states. Such behavior has been predicted theoretically based on n CTMC (Olson *et al.* [22]) and seen experimentally (Abdallah *et al.* [23]) for single ionization.

In conclusion, this experiment presents the first measurement of the average energy and longitudinal momentum of the ejected electrons in multiply ionizing collisions. Also it gives the first experimental determination of the electron average ejection angle as a function of recoil charge state in such collisions. We found that the average energy of electrons increases while the average ejection angle decreases with increasing recoil charge state, and therefore decreasing collision impact parameter. In the transverse direction, the role of the ejected electrons in transverse momentum balance is minimum for large recoil charge states (two-body behavior), but important for low charge states as the projectile suffers small deflection (dipole behavior). The measurements represent an advance in determining the full (vector) momentum distribution of all free particles in atomic collisions and therefore provides a strenuous test of the theoretical understanding of multiply ionizing collisions.

The authors acknowledge C.L. Cocke, W. Wolff, and H. Wolf for useful discussions. This research was supported by the U.S. Department of Energy, Office of Basic Energy Sciences, Division of Chemical Sciences, under Contract No. DE-AC05-96OR22464 with Lockheed Martin Energy Research Corporation. One of the authors (M.A.A.) gratefully acknowledges the support from the ORNL Postdoctoral Research Associates Program administered jointly by Oak Ridge Institute for Science and Education and Oak Ridge National Laboratory.

*Email address: abdallah@mail.phy.ornl.gov

- [1] C.L. Cocke and R.E. Olson, Phys. Rep. **205**, 153 (1991).
- [2] *Atomic Physics: Accelerators*, edited by P. Richard (Academic, New York, 1980).
- [3] R. Moshhammer, J. Ullrich, H. Kollmus, W. Schmitt, M. Unverzagt, O. Jagutzki, V. Mergel, H. Schmidt-Böcking, R. Mann, C.J. Woods, and R.E. Olson, Phys. Rev. Lett. **77**, 1242 (1996).
- [4] M. Schulz, R. Moshhammer, W. Schmitt, H. Kollmus, R. Mann, S. Hagmann, R.E. Olson, and J. Ullrich, J. Phys. B **32**, L557 (1999).
- [5] M. Schulz, R. Moshhammer, W. Schmitt, H. Kollmus, R. Mann, S. Hagmann, R.E. Olson, and J. Ullrich, Phys. Rev. A **61**, 022703 (2000).
- [6] R. Schuch, H. Schöne, P.D. Miller, H.F. Krause, P.F. Dittner, S. Datz, and R.E. Olson, Phys. Rev. Lett. **60**, 925 (1988).
- [7] H. Schöne, R. Schuch, S. Datz, M. Schulz, P.F. Dittner, J.P. Giese, Q.C. Kessel, H.F. Krause, P.D. Miller, and C.R. Vane, Phys. Rev. A **51**, 324 (1995).
- [8] R.E. Olson, J. Ullrich, and H. Schmidt-Böcking, J. Phys. B **20**, L809 (1987).
- [9] R.E. Olson, C.O. Reinhold, and D.R. Schultz, Nucl. Instrum. Methods Phys. Res., Sect. B **53**, 378 (1991).
- [10] R.E. Olson, J. Ullrich, and H. Schmidt-Böcking, Phys. Rev. A **39**, 5572 (1989).
- [11] V. Frohne, S. Cheng, R.M. Ali, M.L.A. Raphaelian, C.L. Cocke, and R. Olson, Phys. Rev. A **53**, 2407 (1996).
- [12] V. Frohne, S. Cheng, R. Ali, M. Raphaelian, C.L. Cocke, and R.E. Olson, Phys. Rev. Lett. **71**, 696 (1993).
- [13] J. Ullrich, R. Moshhammer, R. Dörner, O. Jagutzki, V. Mergel, H. Schmidt-Böcking, and L. Spielberger, J. Phys. B **30**, 2917 (1997).
- [14] J. Borggreen, B. Elbek, and L. Perch Nielsen, Nucl. Instrum. Methods **24**, 1 (1963).
- [15] M.A. Abdallah, C.R. Vane, C.C. Havener, D.R. Schultz, H.F. Krause, N. Jones, and S. Datz (to be published).
- [16] M.A. Abdallah, W. Wolff, H.E. Wolf, E. Sidky, E.Y. Kamber, M. Stöckli, C.D. Lin, and C.L. Cocke, Phys. Rev. A **57**, 4373 (1998); M.A. Abdallah, W. Wolff, H.E. Wolf, E.Y. Kamber, M. Stöckli, and C.L. Cocke, Phys. Rev. A **58**, 2911 (1998).
- [17] D.R. Schultz *et al.*, J. Phys. B **23**, 3839 (1990).
- [18] C.P. Bhalla, N.O. Folland, and M.A. Hein, Phys. Rev. A **8**, 649 (1973).
- [19] P. Jardin, A. Cassimi, J.P. Grandin, D. Hennecart, and J.P. Lemoigne, Nucl. Instrum. Methods Phys. Res., Sect. B **107**, 41 (1996).
- [20] M. Unverzagt, R. Moshhammer, W. Schmitt, R.E. Olson, P. Jardin, V. Mergel, J. Ullrich, and H. Schmidt-Böcking, Phys. Rev. Lett. **76**, 1043 (1996).
- [21] J.C. Levin, R.T. Short, C. Biedermann, H. Cederquist, S.B. Elston, C.-S. O, and I.A. Sellin, Phys. Rev. A **49**, 228 (1994).
- [22] R.E. Olson, C.J. Wood, H. Schmidt-Böcking, R. Moshhammer, and J. Ullrich, Phys. Rev. A **58**, 270 (1998).
- [23] M.A. Abdallah, C.L. Cocke, W. Wolff, H.E. Wolf, and M. Stöckli (to be published).